

**Purdue University**  
**Purdue e-Pubs**

---

Department of Electrical and Computer  
Engineering Faculty Publications

Department of Electrical and Computer  
Engineering

---

2012

# Analysis of thermal conductance of ballistic point contacts

Changwook Jeong

*Birck Nanotechnology Center, Purdue University, jeong.changwook@gmail.com*

Mark S. Lundstrom

*Purdue University, lundstro@purdue.edu*

Follow this and additional works at: <https://docs.lib.purdue.edu/ecepubs>

---

Jeong, Changwook and Lundstrom, Mark S., "Analysis of thermal conductance of ballistic point contacts" (2012). *Department of Electrical and Computer Engineering Faculty Publications*. Paper 145.  
<https://docs.lib.purdue.edu/ecepubs/145>

This document has been made available through Purdue e-Pubs, a service of the Purdue University Libraries. Please contact [epubs@purdue.edu](mailto:epubs@purdue.edu) for additional information.

## Analysis of thermal conductance of ballistic point contacts

Changwook Jeong and Mark Lundstrom

Network for Computational Nanotechnology, Birck Nanotechnology Center, Purdue University,  
West Lafayette, Indiana 47907, USA

(Received 17 April 2012; accepted 16 May 2012; published online 5 June 2012)

Substantial reduction of thermal conductance ( $K_{ph}$ ) was recently reported for air gap heterostructures (AGHs) in which two bulk layers were connected by low-density nanopillars. We analyze  $K_{ph}$  using a full phonon dispersion and including important phonon scattering. We find a transition from ballistic at low temperatures to quasi-ballistic transport near room temperature and explain the slow roll-off in  $K_{ph}$  that occurs near room temperature. We show that the density of nanopillars deduced from the analysis depends strongly on the phonon dispersion assumed. Our model provides a good agreement with experiment that will be necessary to design AGHs for thermoelectric applications. © 2012 American Institute of Physics. [<http://dx.doi.org/10.1063/1.4726111>]

Recently, Bartsch *et al.*<sup>1</sup> demonstrated the fabrication of so-called air-gap heterostructures (AGHs) for which GaAs pillars with controlled length of a few nanometers and diameters of a hundred nanometer are sandwiched between GaAs substrate and capping layers. The thermal conductance of these structures was dramatically reduced in comparison to bulk structures. Bartsch *et al.*<sup>1</sup> explained the measured results with a simple model that assumed pure ballistic transport from low temperatures to room temperature. Since the measurement of thermal conductance ( $K_{ph}$ ) was done for an ensemble of nanopillars, the thermal conductance through a single pillar was not independently measured. Instead, the  $K_{ph}$  for a single pillar was estimated by comparing the measurement to a model calculation for which the transmission was one (i.e., ballistic transport) and a sine-type phonon dispersion was assumed. The pillar density was taken as a fitting parameter, and good agreement was found with the experiment—if the pillar density was assumed to be somewhat larger than expected. In this letter, we report an analysis of the AGH experiment that includes a full description of the phonon dispersion and includes realistic scattering processes. Our analysis supports the simpler analysis by Bartsch *et al.*,<sup>1</sup> but we find that at room temperature, phonon transport through the nanopillars is quasi-ballistic, and the inferred density of nanopillars is significantly lower than that from the simpler analysis. This analysis also explains the slow roll-off in conductance observed experimentally. The results illustrate the importance of including realistic phonon dispersions and scattering when optimizing AGHs for applications such as thermoelectrics.

Heat conduction at length scales comparable to or smaller than phonon mean free paths (MFPs), which can be hundreds of nanometers in crystalline materials at room temperature, has received great attention with the increasing interest in nanostructures. Ballistic transport has been studied in nanostructures such as thin films,<sup>2</sup> nanowires,<sup>3</sup> and superlattices,<sup>4</sup> and the ballistic thermal conductance of an ideal one-dimensional channel has been predicted to have a quantum of thermal conductance,  $k_B^2 T_L \pi^2 / 3h$ .<sup>5,6</sup> Direct evidence of ballistic transport, however, has not been demonstrated in such nanostructures due to non-ideal coupling between thermal reservoirs and thermal conductors, which prevent trans-

mission across two reservoirs from being close to one. Schwab *et al.*<sup>7</sup> addressed this issue by fabricating both reservoirs and conductor from a homogeneous suspended silicon nitride layers and observed the quantum of thermal conductance. Due to the use of a micron-meter long conductor, however, the ballistic thermal conductance was observed only at low temperatures. The work of Bartsch *et al.*<sup>1</sup> shows that ballistic phonon transport (or at least quasi-ballistic, as we shall argue here) can be observed at room temperature.

In this study, we show that: (1) transport should not be considered to be pure ballistic even when the lengths of pillars are well below the average phonon MFP in the bulk material, (2) considering the full phonon dispersion and phonon scattering provides a clear understanding of measured  $K_{ph}$ , which saturates at around 150 K and then roll-offs at room temperature, and (3) the analysis yields a fitted pillar density closer to the measured one. The paper is organized as follows. To calibrate the scattering parameters, we first compare thermal conductivity of bulk GaAs samples to the computed results by using a Landauer approach with a full dispersion description of phonons. Next, we examine quantitatively the effect of sine-type dispersions to demonstrate the importance of the full phonon dispersions—especially in near ballistic transport. Then, we compare thermal conductance without scattering to thermal conductance with scattering to show that pure ballistic transport model holds only at low temperatures. Finally, we show that the computed results match well the experimental data given in Ref. 1. The use of a full dispersion and inclusion of scattering yields a nanopillar density that is significantly lower than the simple model, and it also captures the slow roll-off in conductance for temperatures above 150 K. Finally, we summarize our conclusions.

To determine how close a nanopillar operates to its ballistic limit, the Landauer approach is used because it provides a simple, physically insightful description of ballistic transport and has been widely used to describe quantized electrical and thermal transport in nanostructures. Although not as widely appreciated, the Landauer approach describes diffusive transport as well and provides a simple way to treat the ballistic to diffusive transition. The Landauer formula for thermal conductance ( $K_{ph}$ ) is expressed as<sup>8</sup>

$$K_{ph} = \left( \frac{k_B^2 T_L \pi^2}{3h} \right) \int_0^{+\infty} d(\hbar\omega) (T_{ph} M_{ph}) W_{ph}, \quad (1a)$$

where  $k_B^2 T_L \pi^2 / 3h$  is the quantum of thermal conductance,  $T_{ph}$  is the transmission at a given energy  $\hbar\omega$ ,  $M_{ph}$  is the number of conducting channels at a given energy, and  $W_{ph}$  is a “window function,” which determines the occupation of the channels and is given by<sup>8</sup>

$$W_{ph}(\hbar\omega) = \frac{3}{\pi^2} \left( \frac{\hbar\omega}{k_B T_L} \right)^2 \left( -\frac{\partial n_0}{\partial(\hbar\omega)} \right), \quad (1b)$$

with  $n_0$  being Bose-Einstein distributions. The transmission  $T_{ph}$  is given as<sup>9</sup>

$$T_{ph} = \lambda_{ph}(\omega) / (L + \lambda_{ph}(\omega)), \quad (1c)$$

where  $\lambda_{ph}(\omega)$  is the mean-free-path for backscattering and  $L$  is the length of the conductor, i.e., the length of the pillar in this study. Equation (1a) applies to ballistic limit ( $L \ll \lambda_{ph}(\omega)$ ) for which  $T_{ph} = 1$ , quasi-ballistic regime ( $L \sim \lambda_{ph}(\omega)$ ) for which  $T_{ph} = \lambda_{ph}(\omega) / (L + \lambda_{ph}(\omega))$  as well as to diffusive limit ( $L \gg \lambda_{ph}(\omega)$ ) for which  $T_{ph} = \lambda_{ph}(\omega) / L$ . In the diffusive limit, the Landauer expression for lattice thermal conductivity is equivalent to the conventional expression from BTE.<sup>8</sup>

Given an accurate phonon dispersion,  $M_{ph}(\omega)$  can be readily computed by a simple numerical technique—the “band counting” method.<sup>3,8</sup> To evaluate  $M_{ph}(\omega)$  in this work, a full band description of phonon dispersion of GaAs was obtained from the Tersoff interatomic pair potential model<sup>10</sup> within General Utility Lattice Program (GULP).<sup>11</sup> It is straightforward to compute  $K_{ph}$  per cross-sectional area ( $A$ ) with  $T_{ph} = 1$  in Eq. (1a), i.e., ballistic thermal conductance per area  $K_{ph,BAL}/A$ . A sine-type approximation for phonon dispersion is often used because it provides a compromise between rigorous full phonon dispersions and a simple Debye approximation and is given by<sup>12</sup>

$$\omega = \omega_0 \sin\left(\frac{\pi k}{2k_0}\right), \quad (2)$$

where  $\omega_0$  is the maximum phonon frequency and  $k_0$  is the Debye cutoff wave vector, for which the values are computed as defined in Ref. 12.

Figure 1(a) compares  $M_{ph}$  for a full phonon dispersion to  $M_{ph}$  for a sine-type dispersion. For a sine-type dispersion,  $M_{ph}$  is found to be

$$M_{ph}(\omega) = (3k_0^2 / \pi^3) \arcsin^2(\omega / \omega_0), \quad (3)$$

where the factor of 3 comes from the three phonon polarizations.<sup>13</sup> It is clearly shown in Fig. 1(a) that optical phonon modes are neglected with a sine-type dispersion. For a given  $M_{ph}$ , we first examine diffusive bulk samples to determine the spectral phonon mean-free-path for backscattering,<sup>8</sup>  $\lambda_{ph}(\omega) = (4/3)v_{ph}(\omega)\tau_{ph}(\omega)$ , where  $v_{ph}(\omega)$  is the spectral phonon group velocity at frequency  $\omega$  and  $\tau_{ph}(\omega)$  is the phonon momentum relaxation time. For bulk GaAs samples, the relaxation time approximation (RTA) is used for umklapp

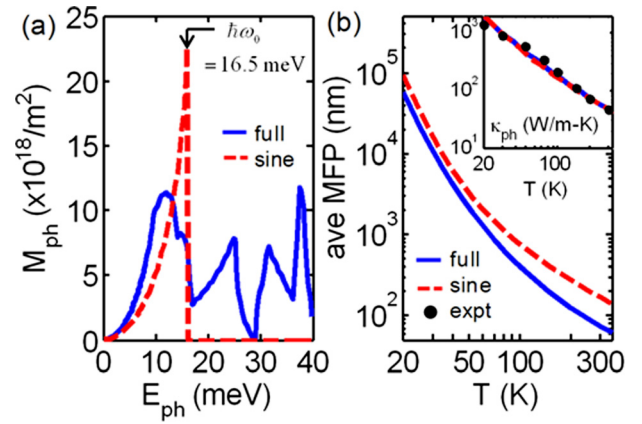


FIG. 1. (a)  $M_{ph}$  is obtained from a full phonon dispersions (solid line) and compared to  $M_{ph}$  from a sine-type dispersion (dashed line) for GaAs.  $\hbar\omega_0 \approx 16.5$  meV represents the maximum cutoff energy for acoustic phonons as defined in a sine dispersion model in Eq. (2). (b) Average MFP as a function of temperature are plotted for the two models of phonon dispersions. A sine-type dispersion model overestimates the average phonon MFP by a factor of 2. Inset: bulk GaAs thermal conductivity vs temperature is plotted using two phonon dispersion models and compared to experiments.

scattering ( $\tau_u^{-1} = B\omega^2 T e^{-C/T}$ ),<sup>14</sup> point defect scattering ( $\tau_d^{-1} = D\omega^4$ ),<sup>15</sup> and crystalline boundary scattering rates ( $\tau_b^{-1} = \text{constant}$ ), where  $B$ ,  $C$ ,  $D$ , and  $\tau_b^{-1}$  are fitted to match the measured data for bulk samples in Ref. 1. The inset of Fig. 1(b) shows that the resulting fit is excellent, regardless of phonon dispersion model. However, it can be seen that a simple sine model overestimates average phonon MFP by a factor of 2, where the average phonon MFP can be obtained by taking the ratio of thermal conductivity ( $\kappa_{ph}$ ) to ballistic thermal conductance per area ( $K_{ph,BAL}/A$ ), as presented in Ref. 8. For example, the average MFP for full phonon dispersion is 72 nm, compared to 166 nm for sine-type dispersion at room temperature. The difference in average MFP can be understood from Fig. 2(a), which compares ballistic thermal conductance per area,  $K_{ph,BAL}/A$ , for a full phonon dispersion to that from a sine-type dispersion. At temperatures higher than 150 K where almost all conducting channels contribute to thermal conduction, neglecting optical

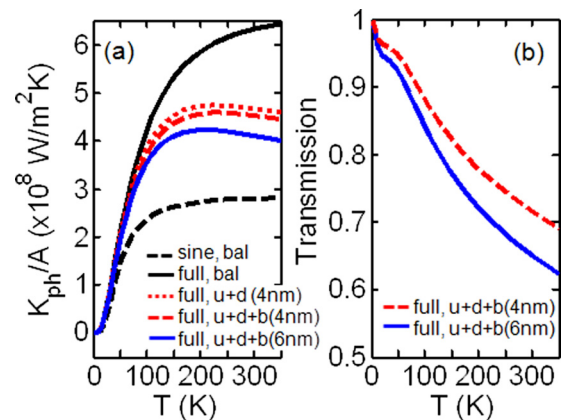


FIG. 2. (a) Computed thermal conductance per area,  $K_{ph}/A$  vs temperature. (b) Average transmission vs temperature. Full: full band dispersion, sine: sine-type dispersion, bal: ballistic assumption, u: umklapp scattering, d: defect scattering, b: boundary scattering. Values in bracket stand for the length of the pillars.

phonon modes within the sine dispersion model leads to  $\sim 2$  times smaller ballistic conductance than that from full dispersion. The  $2\times$  smaller  $K_{ph,BAL}/A$  forces the average phonon MFP to be  $2\times$  larger to match the measured thermal conductivity.

To examine the thermal conductance of the nanopillars, the surface roughness of pillar boundaries should be considered via a frequency-dependent specular parameter. The phonon MFP by the boundary scattering is given by<sup>16</sup>

$$\lambda_b(\omega) = \frac{1 + p(\omega)}{1 - p(\omega)} D_{pillar}, \quad (4)$$

where the diameter of a pillar is  $D_{pillar} = 100\text{ nm}$  as given in Ref. 1, and the specular parameter  $p$  is given by<sup>17</sup>  $p = \exp(-16\pi^3\eta^2/\Lambda_{ph}^2)$ , with  $\Lambda_{ph}$  being the phonon wavelength and  $\eta$  the surface roughness assumed to be  $0.2\text{ nm}$ .<sup>18</sup> For pillars with lengths of  $4\text{ nm}$  and  $6\text{ nm}$ , thermal conductance with scattering and full phonon dispersions is evaluated, as plotted in Fig. 2(a). It is found that the computed thermal conductance per area,  $K_{ph}/A$ , for  $4\text{ nm}$  and  $6\text{ nm}$  long pillars is smaller compared to the pure ballistic thermal conductance, which demonstrates that the nanopillars operate below a fully ballistic limit.

To estimate how close a pillar operates to the ballistic limit, the average transmission is evaluated and presented in Fig. 2(b). The average transmission is defined as the ratio of thermal conductance with scattering being accounted for to ballistic thermal conductance. Figure 2(b) shows that although the transmission at low temperature is indeed close to one, it is reduced to  $0.6\text{--}0.7$  at  $300\text{ K}$ , which clearly illustrates the importance of treating quasi-ballistic transport for the analysis of such nanostructures. Note that the effect of boundary scattering (Eq. (4)) and the length of pillars are negligible; Including boundary scattering reduces  $K_{ph}/A$  only by  $\sim 5\%$  (Fig. 2(a)) and the transmission for  $4\text{ nm}$  pillar is on average about  $7\%$  higher than that for  $6\text{ nm}$  pillar (Fig. 2(b)).

Additional insights can be obtained from Fig. 3, where  $M_{ph}$ ,  $W_{ph}$ , and  $T_{ph}$  in Eq. (1a) vs phonon energy are plotted for three temperatures of  $50$ ,  $150$ , and  $300\text{ K}$ . As the temperature increases, the width of window function ( $W_{ph}$ ) broadens and more conducting channels participate in conduction until the entire spectrum of channels contributes, which occurs at around  $150\text{ K}$ . This results in an increase of thermal conductance with temperature as well as the saturation of thermal conductance for temperatures higher than  $150\text{ K}$ , as shown in Fig. 2(a). In contrast, Fig. 3(b) shows that transmission (Eq. (1c)) keeps decreasing with increasing temperatures mainly due to umklapp scattering. Therefore, thermal conductance with scattering (Fig. 2(a)) roll-offs at  $300\text{ K}$  as the decreasing transmission term takes over the saturated effective number of conducting channels. This effect is not captured in the simple model. Note that as shown in Fig. 3(b), transmission for low energy phonons is close to 1, but high energy phonons have small transmission.

As shown in Fig. 3(a), the increasing importance of optical phonons is clearly visible as temperature increases. To quantitatively examine the contribution of optical phonon modes, Figure 4 shows the cumulative distribution function of thermal conductance as a function of energy with and

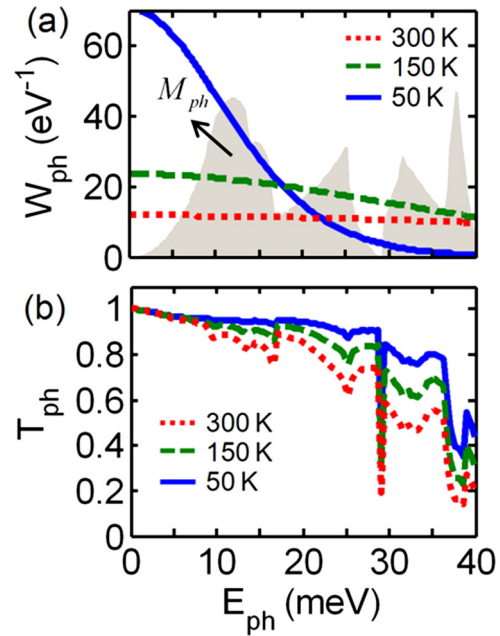


FIG. 3. (a)  $M_{ph}$ ,  $W_{ph}$ , and (b)  $T_{ph}$  are plotted as a function of phonon energy for three temperatures of  $50$ ,  $150$ , and  $300\text{ K}$ .  $M_{ph}$  in Fig. 3(a) is plotted in the units of  $4 \times 10^{17}\text{ m}^{-2}$ .

without scattering for three temperatures of  $50$ ,  $150$ , and  $300\text{ K}$ . At  $50\text{ K}$ , low energy channels (mostly acoustic phonon modes) contribute to more than  $80\%$  of the thermal conductance and two curves obtained with scattering and without scattering almost overlap, which indicates the pillars operate at the near-ballistic limit. At  $150$  and  $300\text{ K}$ , it can be seen that all energy channels contribute to the ballistic thermal conductance and about  $40\text{--}50\%$  of ballistic conduction is carried by optical phonon modes. So a sine dispersion model, which considers only acoustic phonons, should be used with caution for quasi-ballistic transport. It is also

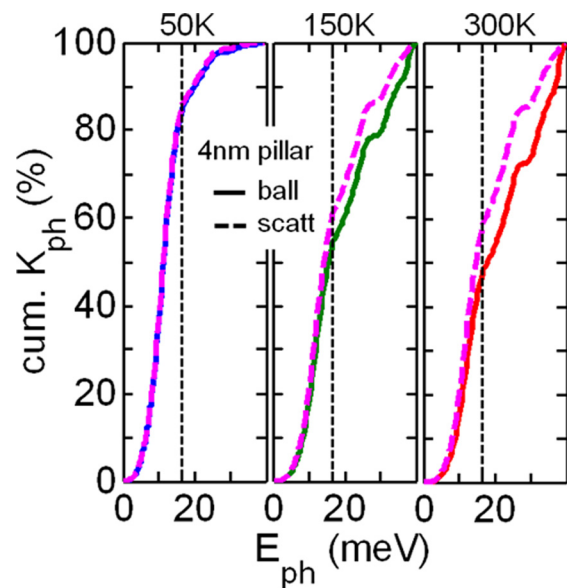


FIG. 4. Cumulative thermal conductance vs energy with scattering (solid line) and without scattering (dashed line) for  $50$ ,  $150$ , and  $300\text{ K}$ . Dotted vertical lines at  $E_{ph} = 16.5\text{ meV}$  represent the cutoff energy for acoustic phonons, as defined in a sine dispersion model (Eq. (2)), and shown in Fig. 1(a). Ball: without scattering, scatt: with scattering.



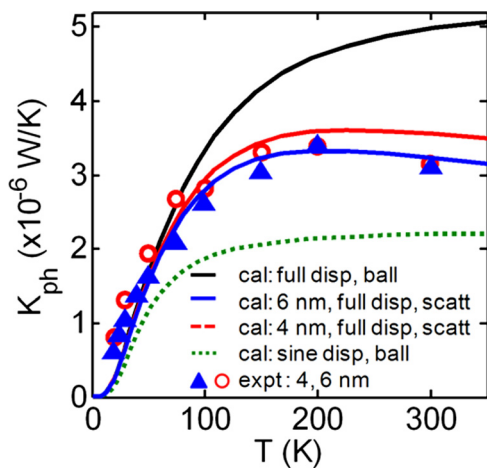


FIG. 5. Computed thermal conductance of a single pillar and experimental data. Full disp: full phonon dispersion, sine disp: sine dispersion, ball: without scattering, scatt: with scattering, 6 nm: 6 nm long pillar, 4 nm: 4 nm long pillar.

observed that with scattering being included, high energy optical phonon modes contribute less to  $K_{ph}$  at high temperatures because optical phonons have short MFPs.

Figure 5 compares computed thermal conductance of a single pillar and the experimental data. The experimental data are calculated by adjusting the pillar densities to match computed  $K_{ph}$ . For the best fit, a sine-type dispersion and pure ballistic model produces a density of  $6.4 \mu\text{m}^{-2}$  for the 4 nm long and  $3.75 \mu\text{m}^{-2}$  for the 6 nm long pillars, as presented in Ref. 1. Using the full phonon dispersion and quasi-ballistic model, best agreement is obtained using a density of  $3.7 \mu\text{m}^{-2}$  for the 4 nm long and  $2.5 \mu\text{m}^{-2}$  for the 6 nm long pillars. Note that these values compare better to the measured density (of a different sample) of about  $2\text{--}3 \mu\text{m}^{-2}$ .<sup>19</sup> The important point is that the pillar density extracted from the analysis depends on the dispersion and scattering models used. Also, it can be seen that calculations with full phonon dispersion and scattering exhibits an excellent agreement with the experimental data at around 300 K, for which a good fit is no longer possible with the pure ballistic model. The results, shown in Fig. 5, demonstrate that considering full phonon dispersion and quasi-ballistic transport is important for the quantitative modeling of thermal transport in nanostructures.

In this paper, we showed that a Landauer approach with full phonon dispersion provides excellent fit to measured thermal conductance of the nanopillar over a wide temperature range with reasonable fitting parameters, i.e., pillar density. We demonstrate that although a sine-type dispersion approximation provides a compromise between rigorous full band and simple Debye models, a full band description of phonon dispersion should be considered in the quasi-ballistic

regime because optical phonons significantly contribute to thermal conduction. Our analysis shows that nanometer long pillars operate below the ballistic limit except for very low temperatures; they deliver about 60% of the ballistic limit at 300 K. Our analysis shows that the measured thermal conductance of pillars in a wide temperature range up to 300 K provides direct evidence of a transition from ballistic to quasi-ballistic transport. An increase of thermal conductance for temperatures lower than  $\sim 150$  K is a signature of ballistic conductance, while a decrease of thermal conductance at  $\sim 300$  K is attributed to reduction in transmission due to strong diffusive scattering. The theoretical framework presented here is important for a clear understanding of fundamental thermal transport in nanostructures and can be useful as a tool for designing AGHs to enhance performance of thermoelectric devices and integrated circuits where the increasing importance of power dissipation, self-heating, and the management of hot spots necessitates rational thermal design.

This work was supported by MARCO Materials Structures and Devices (MSD) Focus Center and computational services were provided by the Network for Computational Nanotechnology (NCN). C.J. acknowledges helpful discussions with J. Maassen.

- <sup>1</sup>Th. Bartsch, M. Schmidt, Ch. Heyn, and W. Hansen, *Phys. Rev. Lett.* **108**, 075901 (2012).
- <sup>2</sup>A. Majumdar, *ASME Trans. J. Heat Transfer* **115**, 7–16 (1993).
- <sup>3</sup>N. Mingo, *Phys. Rev. B* **68**, 113308 (2003).
- <sup>4</sup>G. Chen, *Phys. Rev. B* **57**, 14958 (1998).
- <sup>5</sup>D. E. Angelescu, M. C. Cross, and M. L. Roukes, *Superlattices Microstruct.* **23**, 673–689 (1998).
- <sup>6</sup>L. G. C. Rego and G. Kirczenow, *Phys. Rev. Lett.* **81**, 232 (1998).
- <sup>7</sup>K. Schwab, E. A. Henriksen, J. M. Worlock, and M. L. Roukes, *Nature* **404**, 974–977 (2000).
- <sup>8</sup>C. Jeong, S. Datta, and M. Lundstrom, *J. Appl. Phys.* **109**, 073718–8 (2011).
- <sup>9</sup>S. Datta, *Electronic Transport in Mesoscopic Systems* (Cambridge University Press, 1997).
- <sup>10</sup>D. Powell, M. A. Migliorato, and A. G. Cullis, *Phys. Rev. B* **75**, 115202 (2007).
- <sup>11</sup>J. D. Gale and A. L. Rohl, *Mol. Simul.* **29**, 291–341 (2003).
- <sup>12</sup>C. Dames and G. Chen, *J. Appl. Phys.* **95**, 682–693 (2004).
- <sup>13</sup>We found that sine dispersion model with different cutoff energy for different phonon modes produces similar result to that obtained from sine dispersion model with a single cutoff energy.
- <sup>14</sup>M. Asen-Palmer, K. Bartkowski, E. Gmelin, M. Cardona, A. P. Zhernov, A. V. Inyushkin, A. Taldenkov, V. I. Ozhogin, K. M. Itoh, and E. E. Haller, *Phys. Rev. B* **56**, 9431 (1997).
- <sup>15</sup>M. G. Holland, *Phys. Rev.* **134**, A471–A480 (1964).
- <sup>16</sup>E. H. Sondheimer, *Adv. Phys.* **1**, 1–42 (1952).
- <sup>17</sup>J. M. Ziman, *Electrons and Phonons: The Theory of Transport Phenomena in Solids* (Oxford University Press, New York, 1960).
- <sup>18</sup>Rei Vilar, J. El Beghdadi, F. Debontridder, R. Artzi, R. Naaman, A. M. Ferraria, and A. M. Botelho Do Rego, *Surf. Interface Anal.* **37**, 673–682 (2005).
- <sup>19</sup>Ch. Heyn, A. Stemmann, and W. Hansen, *Appl. Phys. Lett.* **95**, 173110–173110–3 (2009).

## Analysis of thermal conductance of ballistic point contacts

Changwook Jeong and Mark Lundstrom

Citation: [Applied Physics Letters](#) **100**, 233109 (2012); doi: 10.1063/1.4726111

View online: <http://dx.doi.org/10.1063/1.4726111>

View Table of Contents: <http://scitation.aip.org/content/aip/journal/apl/100/23?ver=pdfcov>

Published by the [AIP Publishing](#)

---

### Articles you may be interested in

[Josephson systems based on ballistic point contacts between single-band and multi-band superconductors](#)  
Low Temp. Phys. **41**, 885 (2015); 10.1063/1.4935255

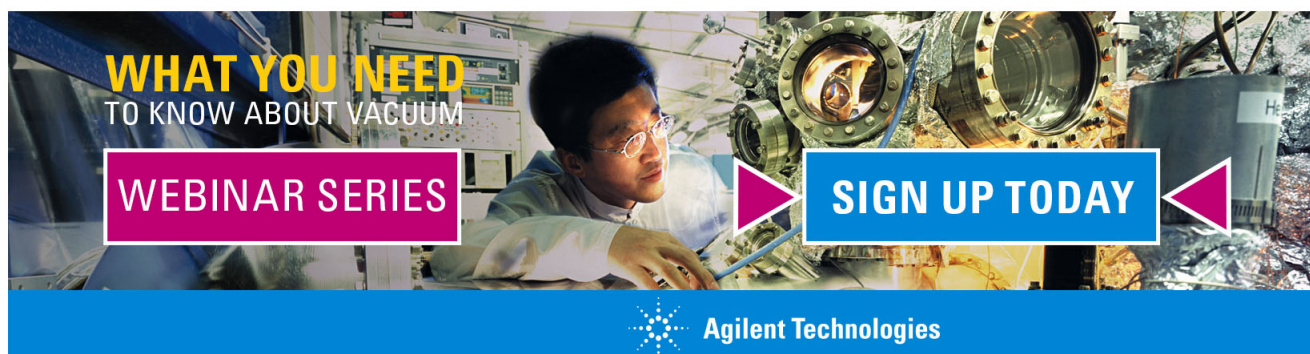
[Ballistic phonon thermal conductance in graphene nanoribbons](#)  
J. Vac. Sci. Technol. B **31**, 04D104 (2013); 10.1116/1.4804617

[Molecular dynamics simulation of thermal transport at a nanometer scale constriction in silicon](#)  
J. Appl. Phys. **101**, 074304 (2007); 10.1063/1.2715488

[Zeeman splitting in ballistic Ga In As/In P split-gate quantum point contacts](#)  
Appl. Phys. Lett. **90**, 122107 (2007); 10.1063/1.2715106

[Low-temperature phonon transport in 3D point-contacts \(Review\)](#)  
Low Temp. Phys. **31**, 921 (2005); 10.1063/1.2127874

---

A promotional banner for a webinar series. It features a background image of a person in a lab coat working with a piece of scientific equipment. The text 'WHAT YOU NEED TO KNOW ABOUT VACUUM' is in yellow and white. Below it, a pink box contains 'WEBINAR SERIES' and a blue box contains 'SIGN UP TODAY'. The Agilent Technologies logo is at the bottom.

**WHAT YOU NEED**  
TO KNOW ABOUT VACUUM

WEBINAR SERIES

SIGN UP TODAY

Agilent Technologies